Digest Journal of Nanomaterials and Biostructures Vol. 8, No. 2, April - June 2013, p. 501 - 511

MODIFICATION OF MULTI-WALL CARBON NANOTUBES FOR THE REMOVAL OF CADMIUM, LEAD AND ARSENIC FROM WASTEWATER

ZLATE S. VELIČKOVIĆ[a]*, ZORAN J. BAJIĆ[a*], MIRJANA Đ. RISTIĆ[b], VELJKO R. DJOKIĆ[b], ALEKSANDAR D. MARINKOVIĆ[b], PETAR S. USKOKOVIĆ[b], MLADEN M. VURUNA[a]

[a]*Military academy, University of Defense, Belgrade, Serbia*

[b]*Faculty of Technology and Metallurgy, University of Belgrade, Serbia*

Multi-wall carbon nanotubes (MWCNTs) was functionalized with 6-arm amino polyethylene glycol (PEG), and synthesized PEG-MWCNTs was used as adsorbent in order to study adsorption characteristics with respect to Cd(II), Pb(II) and As(V) ions. In batch tests, the influence of contact time, initial metal ion concentration and temperature on the ion adsorption on PEG-MWCNTs was studied. Adsorption of Cd(II), Pb(II) and As(V) on PEG-MWCNTs strongly depends on pH. Time dependent adsorption can be described by intra-particular Weber-Morris kinetic model, and adsorption process was modelled by Koble-Corrigan isotherm, respectively. The maximum adsorption capacities of Cd(II), Pb(II) and As(V) on PEG-MWCNTs, for initial concentration of 10 mg dm^{-3} and at pH=4, were 77.6, 47.5 and 13 mg g^{-1} at 25°C, respectively. The competitive adsorption studies showed that the adsorption affinity of ions towards PEG-MWCNTs showed largest adsorption of Cd(II) at pH 8, following by Pb(II) at pH 6, and As(V) at pH 4. Thermodynamic parameters showed that the adsorption of Cd(II), Pb(II) and As(V) ions was spontaneous and endothermic.

(Received January 16, 2013; Accepted March 6, 2013)

Keywords: Cadmium, Lead, Arsenic, Adsorption, Carbon nanotubes, PEG-functionalization.

1. Introduction

Human activities introduce heavy metals and arsenic to the hydrosphere in many ways such as burning of fossil fuels, smelting of ores, municipal sewage, industrial effluent, mining activities, landfill, mineral weathering, underground toxic waste disposal, *etc*. [1] and [2]. These contaminants, regardless of their sources, are easily dispersed into the aquatic system, and tend to accumulate in living organisms, resulting in various disorders and diseases in the ecosystem [3].

Carbon nanotubes (CNTs), developed in the 1990s, possess potential for the removal of many kinds of pollutants from water because of their ability to establish electrostatic interactions and their large surface areas, CNTs have attracted great attention in analytical chemistry and environmental protection. CNTs have shown exceptional adsorption capabilities and high adsorption efficiencies for various organic and inorganic pollutants [4-6].

Modification of the surface morphology plays an important role in enhancing the sorption capacity of CNTs. Due to their high reactivity with many chemical species, it has been suggested that amino groups together with oxygen groups could serve as coordination and electrostatic interaction sites for transition metal sorption [7-10].

In this study, the possibility of the use of PEG-functionalized multi-walled carbon nanotubes (PEG-MWCNTs) as a sorbent for the removal of Cd(II), Pb(II) and As(V) ions from aqueous solutions was examined.

*Corresponding author: zoran.bajic@va.mod.gov.rs

2. Experimental approach

2.1. Materials

All chemicals and MWCNTs were obtained from Sigma-Aldrich. MWCNTs prepared by a chemical vapour deposition (CVD) method were used as received without purification. The purity of MWCNTs was more than 95% and the outer and inner diameters were 20–30, 5–10 nm, respectively, and the length between 5 and 200 μm. All other reagents such as dimethylformamide (DMF), conc. H_2SO_4 (98%) p.a., conc. HNO_3 (65%) p.a., and methanol were used as received. Millipore deionised (DI) water (18 MΩ cm resistivity) was used for sample washing and solution preparation. PEG-6-arm amino polyethylene glycol (PEG-NH_2, Mr ≈15000 g mol^{-1}) (Sunbio, South Korea) was used. Analytical-grade standards: cadmium nitrate (Baker), lead nitrate (Baker) and $Na_2HAsO_4 \cdot 7H_2O$ (Sigma-Aldrich) were employed to prepare a stock solutions containing 1000 mg dm^{-3}, which was further diluted with DI water to the required ionic concentrations for the adsorption experiments.

2.2. Preparation of PEG-MWCNTs

Modification of the raw material was conducted via oxidation, subsequent functionalization with $SOCl_2$ [4], and amination with PEG-NH_2 (Fig. 1).

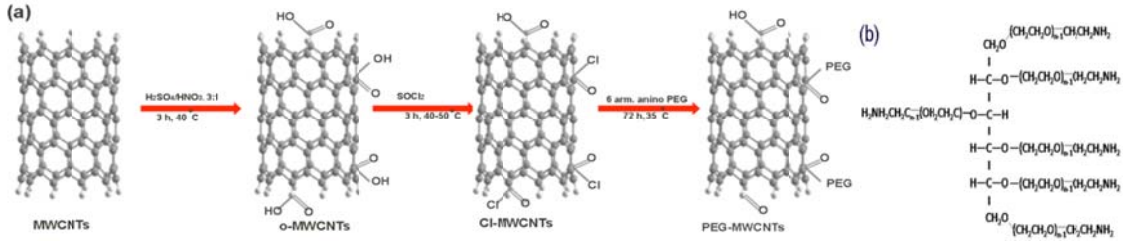

Fig. 1. Reaction pathways applied to obtain PEG-MWCNTs (a), and structure of PEG-6-arm modification agent (b).

The raw-MWCNTs were first treated with a (v/v 3:1) mixture of concentrated H_2SO_4 and HNO_3. This mixture was then sonicated for 3 h at 40°C in an ultrasonic bath to introduce oxygen groups onto the MWCNT surface [11]. Oxidation with sulphuric acid and nitric acid mixture showed better performance than ones oxidized with $KMnO_4$ or H_2O_2 [11,12]. After cooling to room temperature, the oxidized MWCNTs (o-MWCNTs) were added slowly to 300 cm^3 of cold DI water and vacuum-filtered through a 0.05 μm pore size PTFE membrane filter. The filtrate was washed with DI water until the pH was neutral. The sample was dried in a vacuum oven at 80 °C for 8 h. The oxidized nanotubes (90 mg) were dispersed in anhydrous DMF (1 cm^3) in a apparatus protected from the moisture. Thionyl chloride (20 cm^3, Fluka) was added, the dispersion was sonicated for 15 minutes, transferred on a magnetic stirrer and heated at 50 °C for 3 h, and finally the dispersion was heated at 70 °C for 24 h. Obtained product was vacuum filtered with excess anhydrous tetrahydrofuran (THF) (Baker) using a 0.05 μm pore size PTFE membrane filter. Obtained MWCNT-COCl was dried in a vacuum oven at 60 °C for 3 h.

PEG-NH_2 (1.2 g) was dispersed in anhydrous DMF (40 cm^3) in a vials flushed with a nitrogen and protected against moisture. MWCNT-COCl (50 mg) was added into a reaction mixture, and heated at 35 °C, under magnetic stirring, for 72 h. Obtained product was vacuum filtered, dispersed in a 5% $NaHCO_3$ by sonication, and resulting dispersion was centrifuged (two times repeated). After removal of supernatant, precipitate was dispersed in DI water by sonication, and filtered using a 0.05 μm pore size PTFE membrane filter. Extensive washing with DI water and methanol, following by drying in a vacuum oven at 60 °C for 3 h gave a PEG-MWCNTs. Dried PEG-MWCNTs showed significant polymerization degree so it had to be ground for its use in a adsorption experiments.

2.3. Adsorption experiments

Cd(II), Pb(II) and As(V) adsorption capacities of PEG-MWCNTs was determined in a batch reactors. Batch sorption experiments were performed using 100 cm^3 vial with addition of 10 mg PEG-MWCNTs and 100 cm^3 (m/V=100 mg dm^{-3}) of Cd(II), Pb(II), As(V) solution of initial concentrations (C_0) 0.1, 0.5, 1, 2, 5 and 10 mg dm^{-3}. The bottles were placed in an ultrasonic bath. In order to evaluate the effect of pH on adsorption, the initial pH values of the solutions were set at 4.0, 5.0, 6.0, 7.0 and 8.0 by adjustment with 0.01 and 0.1 mol dm^{-3} NaOH, and 0.01 and 0.1 mol dm^{-3} HNO_3, at 25 ºC. The optimal pH was found to be 8 for Cd^{2+}, 6 for Pb^{2+} and 4 for As(V), and these pH was used throughout all the adsorption experiments. Time-dependent sorbate concentration changes were examined in the range 1–240 minutes, and it was found that the optimal time (60 min) was sufficient to achieve equilibration of the system. The mixtures of PEG-MWCNTs and ionic solutions, after sonication was filtered through a 0.2 μm PTFE membrane filter, acidified and analyzed.

2.4. Adsorbent characterization

Fourier-transform infrared (FTIR) spectra were recorded in transmission mode using a BOMEM (Hartmann&Braun) spectrometer. FTIR spectra were recorded before and after adsorption at initial sorbate concentrations of 10 mg dm^{-3}. Samples for FTIR determination were ground with spectral grade KBr in an agate mortar. All FTIR measurements were carried out at room temperature.

JEOL JSM-6390LV scanning electron microscope. Sputtering (with gold) has been performed on BALTEC SCD 005 sputter coater.

Thermogravimetric analysis (TGA) was performed using a TA Instruments SDT Q600 from 20 to 800 °C at a heating rate of 20 °C min^{-1} and a air (200 mL min^{-1}). Elemental analyses were performed using a VARIO EL III Elemental analyser.

The BET specific surface area, pore specific volume and pore diameter were measured by nitrogen adsorption/desorption at 77.4 K using a Micromeritics ASAP 2020MP gas sorption analyzer. The pH values at the point of zero charge (pH_{PZC}) of the samples were measured using the pH drift method [9]. The zeta potential measurements of the PEG-MWCNTs samples were performed using a Zeta-sizer Nano-ZS equipped with a 633 nm He-Ne laser (Malvern). The coordination number (*CN*) can be obtained from the relationship between the concentration of amine groups (DA_{Kaiser} – degree of amination obtained by Kaiser test), and maximum adsorption capacity. Coordination number refers to the number of ligand atoms surrounding the central atom [12].

Cd(II), Pb(II) and As(V) were analyzed by the inductively coupled plasma mass spectrometry (ICP-MS) according to the literature method using an Agilent 7500ce ICP-MS system (Waldbronn, Germany) equipped with an octopole collision/reaction cell, Agilent 7500 ICP-MS ChemStation software, a MicroMist nebulizer and a Peltier cooled (2 °C) quartz Scott-type double pass spray chamber. Standard optimization procedures and criteria specified in the manufacturer's manual were followed.

3. Results and discussion

3.1. PEG-MWCNTs characterization

The FTIR spectra of PEG-MWCNTs, PEG-MWCNTs/Cd(II), PEG-MWCNTs/Pb(II) and PEG-MWCNTs/As(V) are given in Fig. 2. An analysis of FTIR spectra of PEG-MWCNTs shows presence of a weak band at ≈1640 cm^{-1} assigned to stretching of the carbonyl (C=O) overlapping with OH bending vibration. In addition, the bands at ≈1480 and 1150 cm^{-1}, correspond to N–H in-plane and C–N bond stretching vibration, respectively. The broad peaks at 3300–3600 cm^{-1} were due to the NH_2 stretch of the amine group overlapped with OH stretching vibration. A band at ≈800 cm^{-1} was attributed to the out-of-plane NH_2 bending vibration mode [7]. The most intensive peak, after functionalization of MWCNTs with PEG-NH_2, appear at ≈1100 cm^{-1} corresponding to C–O–C stretching vibration from PEG moieties which indicate surface functionality change [8].

Adsorption capabilities of PEG-MWCNTs surface functional groups, as potential binding sites for divalent cations [9,12], depend on the adsorption condition, primarily on solution pH. Divalent cations may form complexes with amino and residual carboxylic and phenolic groups,

more favourable interaction could be expected with former at pH higher than 6 (pKa 3–6), as ionized form could play significant role in uptake of divalent cations. Adsorption capabilities of PEG-MWCNTs with respect to As(V) is higher at lower pH, found pH 4, due to protonation of amino group and more favourable electrostatic interaction with arsenate anion. Characteristics bands of PEG-MWCNTs are slightly shifted, their intensities changed or disappeared after sorption experiments, and this properties depends on sorbate concentrations [9,12].

Bands structure in a spectrum of PEG-MWCNTs treated with Cd and Pb are similar. It could be observed peak shift from ≈1642 cm^{-1} to 1630 cm^{-1} for Cd(II), and 1638 cm^{-1} with Pb(II) indicting influence of cation size and charge density on extent of peak shifting. Peak observed at ≈1383 cm^{-1} is significantly increased, assigned to overlapped stretching vibration of SO_2 and symmetric of COO^-, which reflects to the bond strength increase of these groups after cation adsorption. Also, from Figs. 2 a and b it could be observed that peak at ≈1088 cm^{-1} has shifted and significantly increased. Small intensity increase and shifting are also noted for a peaks at ≈818 and ≈812 cm^{-1} for Cd and Pb, respectively [9,11]. Broad band at ≈3429 cm^{-1} (Fig. 2 a and b), ascribed to OH and NH_2 stretching vibrations, asymmetric and symmetric, is significantly affected by adsorbed divalent cations. New peaks observed in a spectrum of PEG-MWCNTs/Cd(II), appear as a splitting of the band at ≈3429 cm^{-1} giving a slightly resolved peaks at ≈3370 cm^{-1}, ≈3529 cm^{-1} and ≈3631 cm^{-1}. For a lead newly emerged peaks are at ≈3432 cm^{-1} and ≈3450 cm^{-1}. This indicates changes of stretching vibrations of amino and hydroxyl groups due to cadmium and lead ions interaction with electron densities at those groups.

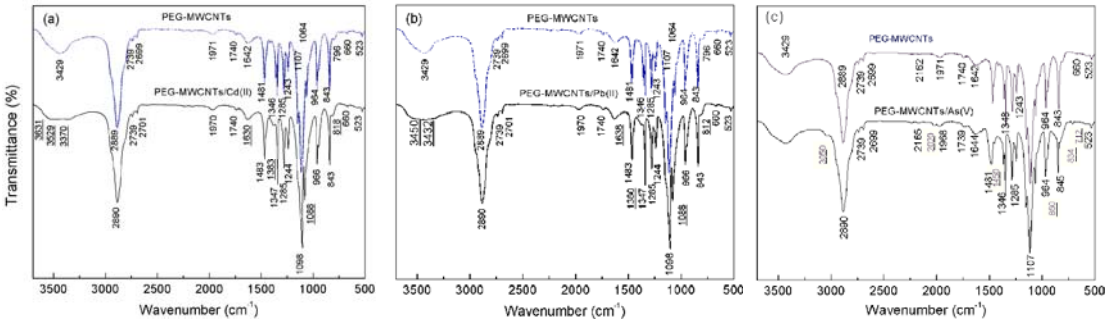

Fig. 2. FTIR spectrum of PEG-MWCNTs, and after treatment in an aqueous solutions (m/V=100 mg dm^{-3}, T=25 ^oC) of (a) Cd(II) ($C[Cd^{2+}]_0$=10 mg dm^{-3}) at pH 8, (b) Pb(II) ($C[Pb^{2+}]_0$=10 mg dm^{-3}) at pH 6, and (c) As(V) ($C[As(V)]_0$=10 mg dm^{-3}) at pH 4.

Analysis of the spectra before and after As(V) adsorption at PEG-MWCNTs could be noted a substantial changes of the stretching vibration frequency of the uncomplexed/unprotonated arsenate anion reflected as a more intense peak at ≈860 cm^{-1} [15], while the frequency of the bonded arsenate has emerged at ≈712 cm^{-1} [13, 14]. Broad band at ≈3429 cm^{-1} (Fig. 2c), ascribed to OH and NH_2 stretching vibrations, asymmetric and symmetric, is not significantly affected by adsorbed arsenic. As a consequence of the amino group protonation, and probably due to interaction with arsenic species, new bands at ≈3050 cm^{-1}, ≈2020 cm^{-1} and 1450 cm^{-1} appeared, indicating that stretching and bending vibrations of ammonium group are influenced by arsenic adsorption.

SEM images show that untreated MWCNTs (Fig 3a) form large aggregates with medium diameter around 5μm due to Van der Waals interactions, while o-MWCNTs (Fig 3b) are not agglomerated because functionalities are mutually repelled by electrostatic forces. Figure 3c and d show that PEG-MWCNTs have polymerized beehive like structure.

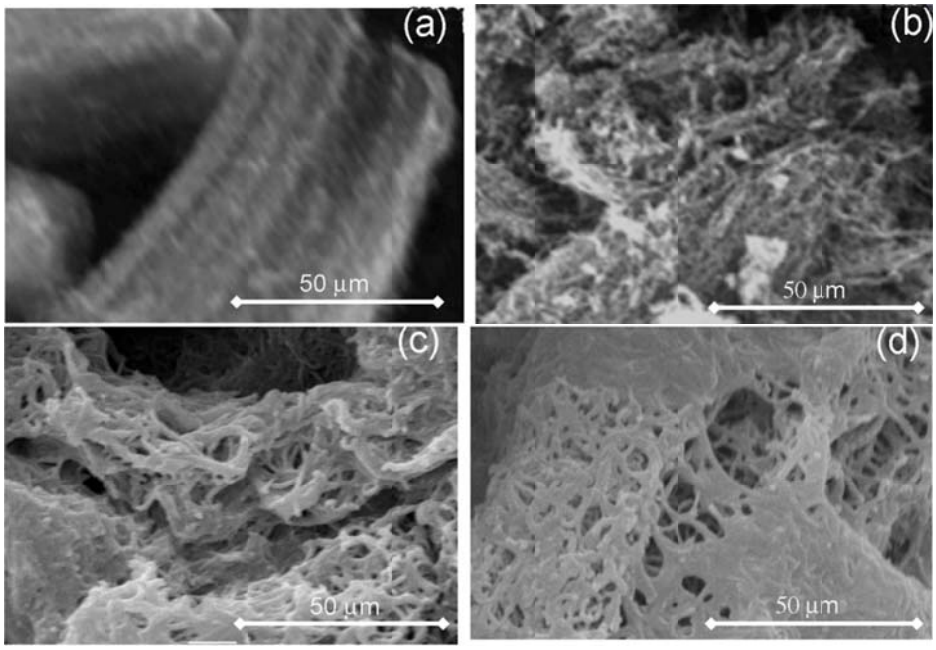

Fig. 3. Comparative overview of SEM images: (a) raw-MWCNTs [7], (b) o-MWCNTs [7], (c) and (d) PEG-MWCNTs.

BET specific surface area and porosity of raw, o-, e- and PEG-MWCNTs, as well as pH_{PZC} and zeta potential are given in Table 1.

Table 1. BET specific surface area and porosity of raw, o-, e- and PEG-MWCNTs .

Adsorbent	Specific surface area (m^2 g^{-1})	Average pore volume (cm^3 g^{-1})	Average pore diameter (nm)	pH_{PZC}	Zeta potential (mV)	Ref.
raw-MWCNT	187.6	0.755	16.09	4.98	-13.7 (pH 5.30)	[9]
o-MWCNT	78.5	0.328	16.72	2.43	-50.0 (pH 3.98)	[9]
e-MWCNT	101.2	0.538	21.25	5.91	-26.9 (pH 6.60)	[9]
PEG-MWCNTs	22.5	0.226	17.40	5.64	-28.4 (pH 6.50)	This study

Results of elemental analysis, DA_{Kaiser} and *CN* values of raw-, o-, e- and PEG-MWCNTs are given in Table 2.

Table 2. Elemental analysis, DA_{Kaiser} and CN values of raw-, o-, e- and PEG-MWCNTs.

Sample	C (%)	H (%)	N (%)	S (%)	DA_{Kaiser} (mmol g^{-1})	*CN*	Ref.
raw-MWCNT	97.46	0.32	0	0	-	-	[9]
o-MWCNT	82.13	1.18	0.49	0.64	-	-	[9]
e-MWCNT	80.08	1.76	4.08	0.58	0.65	3.36	[9]
PEG-MWCNTs	78.22	1.98	5.64	0.12	3.25	4.72	This study

Fig. 4 displays TGA weight-loss curves obtained upon heating o- and PEG-MWCNTs, and gives some information related to thermal stability of functionalities present on MWCNTs surface.

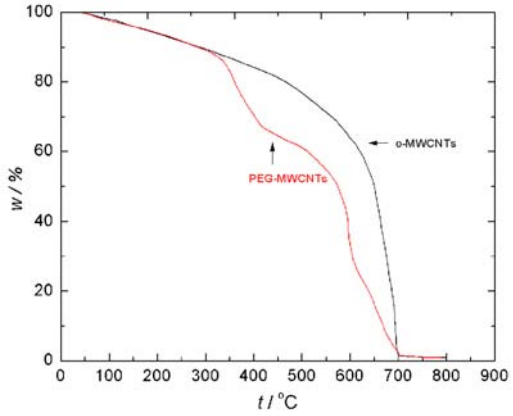

Fig. 4. TGA curves of o- and PEG-MWCNTs.

Peak degradation temperature of o-CNT occurs at 700 °C, and PEG-MWCNTs at 696 °C indicating that amino functionalities are of lower stability (significant loos in the region 300-600 °C), and they could participate in some thermal reactions at temperature >600 °C. Based on the TGA results of PEG-MWCNTs it provides an estimation of 40 wt% attached PEG-NH_2.

3.2. Adsorption kinetics

In order to investigate the kinetics of adsorption of Cd, Pb and As, adsorption kinetic models (pseudo-first order or Lagergren model, pseudo-second order or Ho-McKay model, Roginsky-Zeldovich-Elovich equation and second-order rate equation), and adsorption diffusion models (liquid film linear driving force rate equation, liquid film diffusion mass transfer rate equation, homogeneous solid diffusion model, parabolic or Weber-Morris model, Dunwald-Wagner model and double exponential model) were used [16].

Non-linear regression of experimental data, using Origin 8.0, showed that the best fitting kinetic model is parabolic or Weber-Morris model giving the highest values of correlation coefficients than the other investigated models (Fig. 5). Therefore, this model could be used for the description of the adsorption kinetic of Cd, Pb and As on the PEG-MWCNTs. Weber-Morris found that in many adsorption cases, solute uptake varies proportionally with $t^{1/2}$ rather than with the contact time t [17], according to the equation:

$$q_t = k_p \bullet t^{0.5} + C \tag{1}$$

where k_{int} (g mg^{-1} $min^{-0.5}$) is the intra-particle diffusion rate constant and C is parameter with value other than zero when intra-particle diffusion is not sole rate controlling step and when the film diffusion is simultaneously involved [16].

The curves of Cd(II), Pb(II) and As(V) adsorption exhibited two distinct phases. The first phase (initial steep slope) indicates the instantaneous adsorption of the ions for approximately 30 min. At 30 min., the removal of Cd, Pb and As ions were reached 93.8%, 75.6% and 74.5%, respectively, with the increase in ion uptake less than 0.1% per minute after that period, and equilibrated at 97% for Cd, 78% for Pb, and 76% for As. The steep slope may be attributed to the diffusion of the ions from the aqueous phase to the outer-surface of the PEG-MWCNTs. The initial adsorption has reached equilibrium gradually, exhibiting a classical physisorption process. The second phase exhibits a gradual attainment of equilibrium due to the intra-particle diffusion and low porosity of PEG-MWCNTs (Table 1).

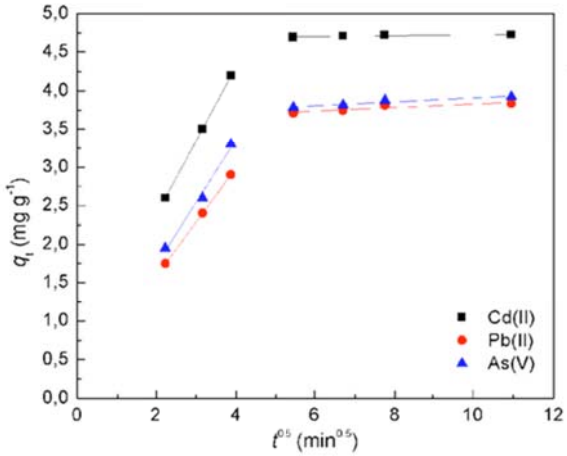

Adsorbate	Cd(II)	Pb(II)	As(V)
k_{int1}	0.977	0.703	0.819
C_1	0.413	0.179	0.0867
R_1^2	0.999	0.999	0.990
k_{int2}	0.00508	0.0256	0.0225
C_2	4.67	3.65	3.60
R_2^2	0.863	0.913	0.837

Fig. 5. Kinetic plot of experimental data and calculated parameters of the first and second phase for the Weber-Morris intra-particle model for Cd(II), Pb(II), As(V) adsorption on PEG-MWCNTs.

3.4. Adsorption isotherms

Many adsorption isotherm models were used in order to describe adsorption process, and to calculate various adsorption parameters according to: Langmuir, Freundlich, Sips, Jovanovic, Jovanovic-Freundlich, Dubinin–Radushkevich, Dubinin-Astakhov, Radke-Prausnitz, Redlich-Peterson, Temkin, Koble-Corrigan (K-C) and Fritz-Schlünder isotherm. It was found that the best fitting data were obtained using Koble-Corrigan and Freundlich isotherms (Figs. 6 and 7).
Koble–Corrigan isotherm [18] is a three-parameter equation, which incorporated both Langmuir and Freundlich isotherm models for representing the equilibrium adsorption data for heterogeneous adsorption surfaces.

$$q_e = \frac{aC_e^n}{1+bC_e^n} \tag{2}$$

The isotherm constants, a, b and n are calculated from the nonlinear regression fitting of experimental data. Freundlich isotherm [19] is widely applied in heterogeneous systems especially for organic compounds or highly interactive species on activated carbon and molecular sieves.

$$q_e = k_f C_e{}^n \text{, and linearized form } \log q_e = \log k_f + n \log C_e \tag{3}$$

The slope ranges between 0 and 1 is a measure of adsorption intensity or surface heterogeneity, becoming more heterogeneous as its value gets closer to zero. Whereas, a value below unity implies chemisorptions process, while n above one is an indication of cooperative adsorption [20]. Langmuir model is used for calculation thermodynamic parameters of adsorption process.

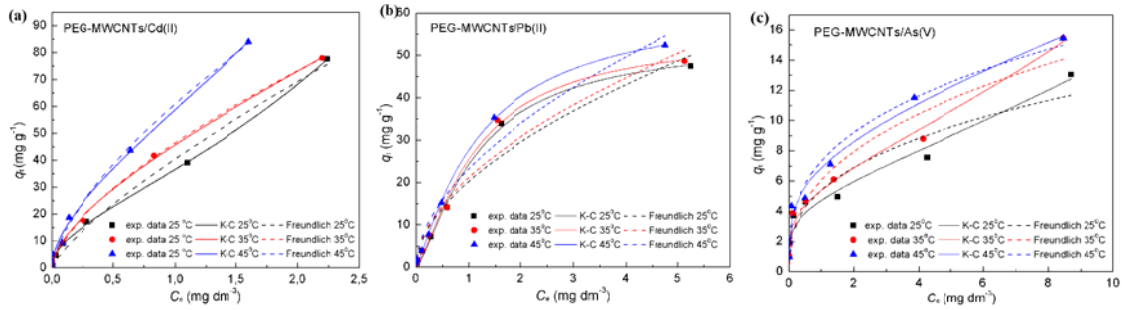

Fig. 6. Freundlich adsorption isotherms of Cd(II) at pH 8 (a), Pb(II) at pH 6 (b), and As(V) at pH 4 (c) on the PEG-MWCNTs at 25, 35 and 45 °C. (C_0 = 0.10, 0.20, 0.50, 1.0, 2.0, 5.0, and 10.0 mg dm^{-3}, m/V = 100 mg dm^{-3}).

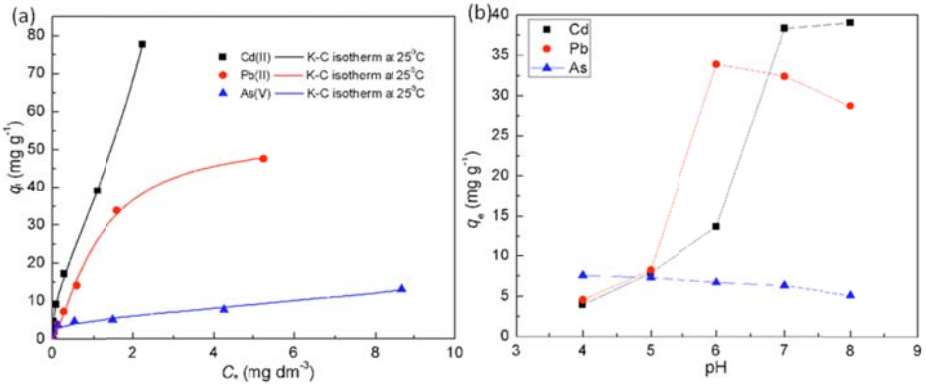

Fig. 7. (a) Koble-Corrigan isotherms for adsorption of Cd(II) and Pb(II) at pH 6, and As(V) at pH 4 on the PEG-MWCNTs at 25 °C. (C_0 = 0.10, 0.20, 0.50, 1.0, 2.0, 5.0, and 10.0 mg dm^{-3}, m/V = 100 mg dm^{-3}), (b) Effect of pH on adsorption of Cd(II), Pb(II) and As(V) on the PEG-MWCNTs (C_0 = 5 mg dm^{-3}, m/V = 100 mg dm^{-3}, T = 25 °C).

The results of experimental data fitting to Koble-Corrigan and Freundlich isotherms, using nonlinear method, are given in Table 3.

Table 3. Adsorption isotherms parameters for Cd(II), Pb(II) and As(V) removal on PEG-MWCNTs.

Isotherm	Cd(II)			Pb(II)			As(V)		
	25°C	35°C	45°C	25°C	35°C	45°C	25°C	35°C	45°C
Koble-Corrigan									
a ((dm^3 mg^{-1})^n)	19.07	40.58	40.96	44.58	47.31	49.56	0.8543	0.9894	3.568
b ((dm^3 mg^{-1})^n)	-0.478	-0.112	-0.303	0.829	0.855	0.787	-0.818	-0.815	-0.478
n	0.399	0.584	0.501	1.362	1.344	1.185	0.056	0.059	0.162
R^2	0.999	0.996	0.993	0.996	0.994	0.998	0.977	0.989	0.987
Freundlich									
K_F ((mg g^{-1}) (dm^3 mg^{-1})$^{1/n}$)	40.44	46.49	60.92	20.31	21.21	23.25	5.371	6.033	7.289
n	1.288	1.523	1.498	1.842	1.857	1.827	2.784	2.523	2.960
R^2	0.990	0.996	0.994	0.956	0.955	0.965	0.921	0.938	0.974

Results suggest that adsorption of Cd(II), Pb(II), As(V) on PEG-MWCNTs is best modelled using Koble-Corrigan isotherm. The maximum adsorption of investigated ions obtained experimentally was given in Table 4.

Values of $n > 1$ indicate that adsorption processes slightly decreased at lower sorbate concentration, and also indicates on presence of different active centres where the highest energies ones is of higher activity, *e.g.* participate in a initial adsorption step. Also, values higher than 1 indicates that cooperative mechanism, *i.e.* physisorption and chemisorption, are operative having different contribution at different phase of system equilibration.

Table 4. Experimental values of Cd(II), Pb(II) and As(V) uptake on PEG-MWCNTs at 25°C.

Initial concentration (mg dm^{-3})	Cd(II), pH 8		Pb(II), pH 6		As(V), pH 4	
	q_e (mg g^{-1})	% of removal	q_e (mg g^{-1})	% of removal	q_e (mg g^{-1})	% of removal
0.1	0.991	99.1	0.840	84.0	0.979	97.9
0.2	1.96	98.0	1.66	83.1	1.87	93.6
0.5	4.72	94.4	3.78	75.7	3.71	74.3
1	9.08	90.8	7.20	72.0	4.61	46.1
2	17.1	85.6	14.08	70.4	4.94	24.7
5	39.0	78.0	33.9	67.8	7.56	15.1
10	77.6	77.6	47.5	47.5	13.0	13.0

3.5. Error functions

In order to measure the quality of fitting the validation of adsorption isotherms were accomplished using different error functions alongside with the correlation coefficient R^2. Using nonlinear regression instead of linear incorporates the minimization or maximization of error distribution between the experimental data and the predicted isotherms based on its convergence criteria [21]. The data analysis was accomplished using Marquardt's percent standard deviation (MPSD); hybrid fractional error function (HYBRID); average relative error (ARE); average relative standard error (ARS); sum squares error (ERRSQ/SSE); normalized standard deviation (NSD); standard deviation of relative errors (s_{RE}); spearman's correlation coefficient (r_s) and nonlinear chi-square test (χ^2) (Table 5).

Table 5. Values of correlation coefficients and error functions for Cd(II), Pb(II) and As(V) adsorption on PEG-MWCNTs for K-C and Freundlich isotherms.

	Cd(II)		Pb(II)		As(V)	
	K-C	F	K-C	F	K-C	F
R^2	0.973	0.971	0.995	0.955	0.989	0.939
MPSD	45.76	50.22	57.72	90.16	25.47	40.37
HYBRID	84.45	84.73	59.33	179.5	11.55	38.54
ARE	23.63	28.77	31.44	57.61	12.02	26.98
ARS	0.3736	0.4584	0.471	0.823	0.2079	0.3686
ERRSQ	19.34	20.19	11.30	93.40	1.581	8.857
NSD	37.36	45.84	47.13	82.31	20.79	36.86
s_{RE}	25.05	30.38	33.53	63.09	12.96	28.90
r_s	0.9232	0.9199	0.955	0.629	0.9937	0.9649
χ^2	3.378	4.237	2.373	8.976	0.4619	1.927

3.3. Adsorption thermodynamics

The Gibbs free energy (ΔG^0), enthalpy (ΔH^0) and entropy (ΔS^0) of adsorption were calculated using the Van't Hoff thermodynamic equations:

$$\Delta G^0 = -RT\ln(b) \tag{4}$$

$$\ln(b) = \Delta S^0 / R - \Delta H^0 / (RT) \tag{5}$$

where b is nondimensional Langmuir constant, T is the absolute temperature in K and R is the universal gas constant (8.314 J mol^{-1} K^{-1}). ΔH^0 (kJ mol^{-1}) and ΔS^0 (J mol^{-1} K^{-1}) can be obtained from the slope and intercept of ln(b) versus 1/T plot, assuming the sorption kinetics to be under steady-state conditions. The calculated thermodynamic values (Table 6) provide information on the adsorption mechanism.

Table 6. Calculated Gibbs free energy of adsorption, enthalpy and entropy for Cd(II), Pb(II) and As(V) adsorption on PEG-MWCNTs at 298, 308 and 318 K.

	ΔG^0			ΔH^0	ΔS^0
	298 K	308 K	318 K		
Cd(II)	-39.52	-41.66	-43.71	21.98	209.8
Pb(II)	-42.11	-44.24	-46.15	17.04	201.9
As(V)	-45.02	-47.62	-49.83	25.50	240.8

The negative adsorption standard free energy changes (ΔG^0) (kJ mol^{-1}) and positive standard entropy changes (ΔS^0) at all temperatures indicate that the adsorption reactions are spontaneous. For both sorbents the adsorption is endothermic (ΔH^0 is positive). The decrease of Gibbs free energy (ΔG^0) with increasing temperature indicates that spontaneity of the reaction increases.

5. Conclusions

The applicability of the isotherm equation to describe the adsorption process was judged by the correlation coefficients and error functions. Thus, the adsorption isotherm models fitted the data better by the use of Koble–Corrigan isotherm. Adsorption kinetic studies showed that the best fitting kinetic model is parabolic or Weber-Morris model giving the highest values of correlation coefficients than the other investigated models. Therefore, this model could be used for the prediction of the kinetics of adsorption of Cd, Pb and As on the PEG-MWCNTs. The adsorption properties of raw-MWCNTs were significantly improved by amino-functionalization, and modification of nanotubes using PEG generated novel material suitable for removal of heavy metal and metalloid species from water. Chemical modification of MWCNTs with PEG-NH_2 offers an alternative to produce of filtration membranes for the removal of heavy metals from industrial waters at higher temperatures, and for preconcentration of heavy metals in analytical chemistry and environmental protection.

Acknowledgment

Financial support through the Ministry of Education, Science and Technological development of the Republic of Serbia, Project No. 172013, is gratefully acknowledged.

References

[1] W. Salomons, U. Förstner, P. Mader, (1995). Heavy Metals Problems and Solutions, Springer, New York .
[2] D. Mohan, C. U. Pittman Jr., J. Hazard. Mater., 142, 1–53 (2007).
[3] F. Miculescu, M. Miculescu, L. T. Ciocan, A. Ernuteanu, I. Antoniac, I. Pencea, E. Matei, Digest J. Nanom. Biostruct. **6** (3), 1117-1127 (2011).
[4] M. O'Connell, (2006). Carbon nanotubes: properties and applications, Ch. 8, CRC Press Taylor & Francis Group, Boca Raton, FL, USA.
[5] S. Iijima, Nature **354**, 56-58 (1991).
[6] L. M. Dai, A.W.H. Mau, Adv. Mater. **13**, 899-913 (2001).
[7] G. Vuković, A. Marinković, M. Obradović, V. Radmilović, M. Čolić, R. Aleksić, P.S. Uskoković, Appl. Surf. Sci. **255**, 8067-8075 (2009).
[8] M.J. Kim, J. Lee, D. Jung, S.E. Shim, Syntetic metals, **160**, 1410-1414 (2010).
[9] G.D. Vuković, A.D. Marinković, M. Čolić, M.Đ. Ristić, R.A. Aleksić, A. Perić-Grujić, P.S. Uskoković, Chem. Eng. J. **157**, 238–248 (2010).
[10] M. A. Tofighy, T. Mohammadi, J. of Haz. Mat. **185**, 140–147 (2011).
[11] N. A. Buang, F. Fadil, Z. A. Majid, S. Shahir, Digest J. Nanom. Biostruct. **7**(1), 33-39 (2012)
[12] G. D. Vuković, A. D. Marinković, S. D. Škapin, M. Đ. Ristić, R. Aleksić, A. A. Perić-Grujić, P. S. Uskoković, Chem. Eng. J. **173**(2011) 855– 865.
[13] S. Myneni, S. Traina, G. Waychunas, T. Logan, Geochim. Cosmochim. Acta.**, 62**, 3285-3300 (1998).
[14] Z. Veličković, G. D. Vuković, A. D. Marinković, M. S. Moldovan, A. A. Perić- Grujić, P.S. Uskoković, M. Đ. Ristić, Chem. Eng. J.**, 181-182**, 174- 181 (2012).
[15] S. Goldberg, C. T. Johnston, J. Colloid. Interface Sci.**, 234**, 204–216 (2001).
[16] H. Qiu, L. LV, B. Pan, Q. Zhang, W. Zhang, Q. Zhang, J. Zhejiang Univ Sci A **10**(5), 716-724 (2009)
[1] W. J. Weber, J. C. Morris, Sanit. Eng. Div., ASCE **89** (SA2), 31–59 (1963).
[2] R. A. Koble, T. E. Corrigan, Ind. Eng. Chem. **44**, 383–387 (1952).
[3] H. M. F. Freundlich, J. Phys. Chem. **57**, 385–471 (1906).
[4] F. Haghseresht, G. Lu, Energy Fuels **12**, 1100–1107 (1998).
[5] K.Y. Foo, B.H. Hameed, Chem. Eng. J. **156**, 2–10 (2010).